OPEN ACCESS Freely available online

PLOS ONE

Design of High-Specificity Nanocarriers by Exploiting Non-Equilibrium Effects in Cancer Cell Targeting

Konstantinos Tsekouras[1], Igor Goncharenko[1], Michael E. Colvin[2], Kerwyn Casey Huang[3]*, Ajay Gopinathan[1]*

1 Department of Physics, University of California Merced, Merced, California, United States of America, **2** Department of Chemistry and Biochemistry, University of California Merced, Merced, California, United States of America, **3** Department of Bioengineering, Stanford University, Stanford, California, United States of America

Abstract

Although targeting of cancer cells using drug-delivering nanocarriers holds promise for improving therapeutic agent specificity, the strategy of maximizing ligand affinity for receptors overexpressed on cancer cells is suboptimal. To determine design principles that maximize nanocarrier specificity for cancer cells, we studied a generalized kinetics-based theoretical model of nanocarriers with one or more ligands that specifically bind these overexpressed receptors. We show that kinetics inherent to the system play an important role in determining specificity and can in fact be exploited to attain orders of magnitude improvement in specificity. In contrast to the current trend of therapeutic design, we show that these specificity increases can generally be achieved by a combination of low rates of endocytosis and nanocarriers with multiple low-affinity ligands. These results are broadly robust across endocytosis mechanisms and drug-delivery protocols, suggesting the need for a paradigm shift in receptor-targeted drug-delivery design.

Citation: Tsekouras K, Goncharenko I, Colvin ME, Huang KC, Gopinathan A (2013) Design of High-Specificity Nanocarriers by Exploiting Non-Equilibrium Effects in Cancer Cell Targeting. PLoS ONE 8(6): e65623. doi:10.1371/journal.pone.0065623

Editor: Bing Xu, Brandeis University, United States of America

Received January 8, 2013; **Accepted** April 25, 2013; **Published** June 26, 2013

Funding: The authors acknowledge support from National Science Foundation grant EF-1038697. AG also acknowledges support from a James S. McDonnell Foundation Award, a University of California Institute for Mexico and the United States (UC MEXUS) grant, and a George E. Brown, Jr. Award. The funders had no role in study design, data collection and analysis, decision to publish, or preparation of the manuscript.

Competing Interests: The authors have declared that no competing interests exist.

* E-mail: kchuang@stanford.edu (KCH); agopinathan@ucmerced.edu (AG)

Introduction

Collateral damage to healthy tissues caused by therapeutic agent action remains a major problem for cancer therapy, limiting treatment efficacy and applicability, and ultimately compromising patient survival. Specificity can be enhanced via therapeutic agent-containing nanocarriers equipped with ligands that bind receptors selectively overexpressed in cancer cells [1–3]. Although this approach holds promise, with a number of drugs on the market [4] and ongoing research focusing on nanocarrier-ligand conjugates and on identifying viable receptors [5–8], the occurrence of side effects in nanocarrier-treated patients remains a limiting factor. The rational design of multivalent nanocarriers for optimal specificity therefore presents an intriguing and important challenge.

Several recent theoretical and experimental studies [9–15] have been motivated by the relevance of multivalent ligand-receptor binding for both nanocarrier design and biological processes such as immune system function. In the context of high-specificity cancer cell targeting, it has been shown that multivalent nanocarriers equipped with low-affinity ligands can achieve much higher coverage on cells with modestly higher receptor densities under equilibrium conditions [3,16]. However, it is the number of nanocarriers internalized that is of therapeutic consequence and not merely the number in contact with the cell surface under idealized conditions of equilibrium. We expect then that specificity will be governed by the different time scales associated with endocytosis, ligand-receptor binding/unbinding, and the method of drug delivery. Even when one considers simple linear response near equilibrium, it has been found that the magnitude of the endocytosis rate sets the maximal specificity [3], pointing to the critical importance of kinetics. In fact, we find that both the magnitude of the endocytosis rate and its functional dependence on the number of bound ligands, which is governed by the molecular mechanism of endocytosis, have substantial effects on the specificity.

Furthermore, equilibrium-based studies cannot address different drug-delivery protocols, as these create time-dependent nanocarrier availabilities and thus preclude the existence of a steady state. In any event, a steady state is virtually impossible to achieve *in vivo*, where natural biological cycles, homeostasis mechanisms, and the practicalities of drug-administration regulations all conspire against it. We explore these issues with an approach examining the *kinetics* of nanocarrier-ligand complexes binding to healthy and cancer cells so as to identify drug design strategies that maximize targeting specificity. We show that there exist peaks in the specificity as a function of both affinity and number of ligands, implying the existence of optimal nanocarrier designs with a large number of very weakly binding individual ligands with ligand-receptor dissociation constants in the mM range. We further demonstrate that specificity can be increased by orders of magnitude by exploiting the kinetics of the system via targeting receptors that are slowly endocytosed only in groups and/or by a judicious tuning of the time dependence of drug delivery. Remarkably, the optimal design region of parameter space shows little variation even among significantly different drug-delivery

protocols and endocytosis mechanisms, pointing to the existence of robust design principles.

Methods

We construct a minimal kinetic model for the endocytosis of nanocarriers equipped with N ligands (Fig. 1). Ligands independently bind to and unbind from individual receptors with rates k_+, k_- for healthy cells and αk_+, k_- for cancer cells, where α is the factor by which cancer cells overexpress receptors. The values of these rates depend on a variety of factors such as nanocarrier size and ligand/receptor type, and can be related to standard chemical kinetics constants by noting that $k_{off}=k_-$ and $k_{on}=k_+/C_0$, where C_0 is the effective receptor concentration in the vicinity of a single ligand (File S1) and it is assumed that there is a large excess of mobile receptors. Therefore $K_d=K_a^{-1}=k_{off}/k_{on}=C_0k_-/k_+$, where K_d is the dissociation constant and K_a is the ligand-receptor affinity constant. The independence of the ligand binding, while assumed for simplicity, is a good approximation for many multivalent supramolecular interactions [17]. Nanocarriers enter the system with an input rate, $I(t)$, determined by the *drug-delivery protocol*, which is the method whereby the treatment is administered and the kinetics of first binding of the nanocarriers to the cell surface. We examined three cases: (i) the steady state arising from a constant supply of nanocarriers, (ii) the result of a single, high-concentration dose, and (iii) pretargeted delivery in which a ligand complex is introduced first (at $t=0$) and then followed later by the active therapeutic (at $t=t_1$), which docks with nanocarriers remaining in the system. For this last protocol, we measured specificity for a given *collection time window* $\Delta t=t_2-t_1$, where t_2 is set by physiological time scales and corresponds to the time beyond which endocytosis of activated therapeutic-nanocarrier complexes is negligible. After attaching to a cell, nanocarriers are removed from the system if all ligands unbind (we do not consider nanocarrier "recycling") or if they are endocytosed. Endocytosis occurs with a rate $k_e(n)$, whose dependence on the number n of bound ligands we term the *endocytosis profile*.

Each nanocarrier can then be represented by a 1D random walker on the discrete interval $[0,N]$ between an absorbing barrier at 0 and a reflecting barrier at N, with a rate $k_e(n)$ of particle loss at each site n (Fig. 1B). At time t, a walker at position n represents a nanocarrier with n ligands bound. Denoting the probability that a nanocarrier has n ligands bound at time t as $P_n(t)$, we derived master equations for a nanocarrier attached to a healthy cell:

for $1<n<N$,

$$\frac{dP_n(t)}{dt}=-[(N-n)k_++nk_-]P_n(t)+(n+1)k_-P_{n+1}(t) +(N-n+1)k_+P_{n-1}(t)-k_e(n)P_n(t); \quad (1)$$

for $n=N$,

$$\frac{dP_N(t)}{dt}=-Nk_-P_N(t)+k_+P_{N-1}(t)-k_e(N)P_N(t); \quad (2)$$

for $n=1$,

$$\frac{dP_1(t)}{dt}=-[(N-1)k_++k_-]P_1(t)+2k_-P_2(t)+I(t)-k_e(1)P_1(t). \quad (3)$$

For a nanocarrier attached to a cancer cell, k_+ in Eqs. 1–3 is simply replaced by αk_+.

This system of master equations can be recast as the vector equation

$$\frac{\partial \mathbf{P}(t)}{\partial t}=\mathbf{M}\mathbf{P}(t), \quad (4)$$

where the n^{th} component of $\mathbf{P}(t)$ is $P_n(t)$ and the elements of the matrix $\mathbf{M}$ are dictated by the appropriate coefficients in the master equations. Eq. 4 can then be solved numerically, with initial conditions $P_n(0)=0$, to determine the eigenvectors and eigenvalues for various combinations of endocytosis profiles, drug-delivery protocols, and values of α, N, k_+, and (for pretargeted drug delivery) collection time windows Δt. For each combination of drug-delivery protocol and endocytosis profile we determined the specificity, $S=\alpha^{-1}E_c/E_h$, where E_c and E_h are the numbers of nanocarriers endocytosed by cancer and healthy cells, respectively. E_c and E_h can be computed as the integral over the relevant time window of the net rate of drug internalization, $\sum_{n=1}^{N}k_e(n)P_n(t)$. The factor α^{-1} in the equation for S normalizes for the increased number of receptors on the cancer cell. In addition to determining the full numerical solutions for all combinations, we validated all results with Monte Carlo simulations using the Gillespie algorithm. Furthermore, we derived an analytical solution for the combination of a constant endocytosis profile at steady state in the limit $k_+\gg k_-$ that agrees with our numerical results (File S1).

Results

Specificity peaks for high numbers of weakly bound ligands

To investigate the role of kinetic effects on the specificity, we first examined the impact of varying endocytosis profiles for a fixed steady-state drug-delivery protocol. We are interested in how the specificity S depends on the following subset of nanocarrier design parameters: the ligand number N and the ligand-receptor affinity constant K_a. Fig. 2A displays the specificity for a constant endocytosis profile, where $k_e(n)=k_e^c$. There is a well defined range of optimal design parameters where the specificity is substantially higher than the surroundings. Locally optimal solutions appear in a continuous curve ranging from small peaks at $N=2$ for large K_a ($k_+\gg k_-$) to large peaks at large N for $k_+\sim k_-$.

In general, for reasonable values of k_e^c and α (Table 1), we find that specificity peaks globally for high numbers of ligands and a dissociation rate K_d on the order of mM (Fig. 2A). This can be understood in terms of the relative values of the single ligand on and off rates. If $k_+>k_-$, nanocarriers will bind to both healthy and cancer cells, while if $k_+\ll k_-$ nanocarriers will bind to neither cell type; both effects reduce specificity. If $k_+<k_-$, nanocarriers on healthy cells remain more likely to unbind than to bind a ligand; however, if k_+ is close to k_- such that $\alpha k_+>k_-$, then nanocarriers on cancer cells will be more likely to bind than to unbind a ligand. Thus, in this regime, ligand binding selects for nanocarriers bound to cancer cells, and the desired bias increases as this pre-selected population feeds into the next ligand-binding reaction. Therefore, on average nanocarriers spend more time bound to cancer cells compared with healthy cells and thus have a higher likelihood of being endocytosed. For very large K_a, nanocarriers strongly prefer to bind rather than unbind a ligand irrespective of whether they are bound to healthy or cancer cells, giving a very high probability that a nanocarrier is nonspecifically endocytosed. This probability increases with the number of ligands, leading to the specificity decreasing and tending to 1 (the lower bound) in the large N limit. The specificity at $N=1$ is

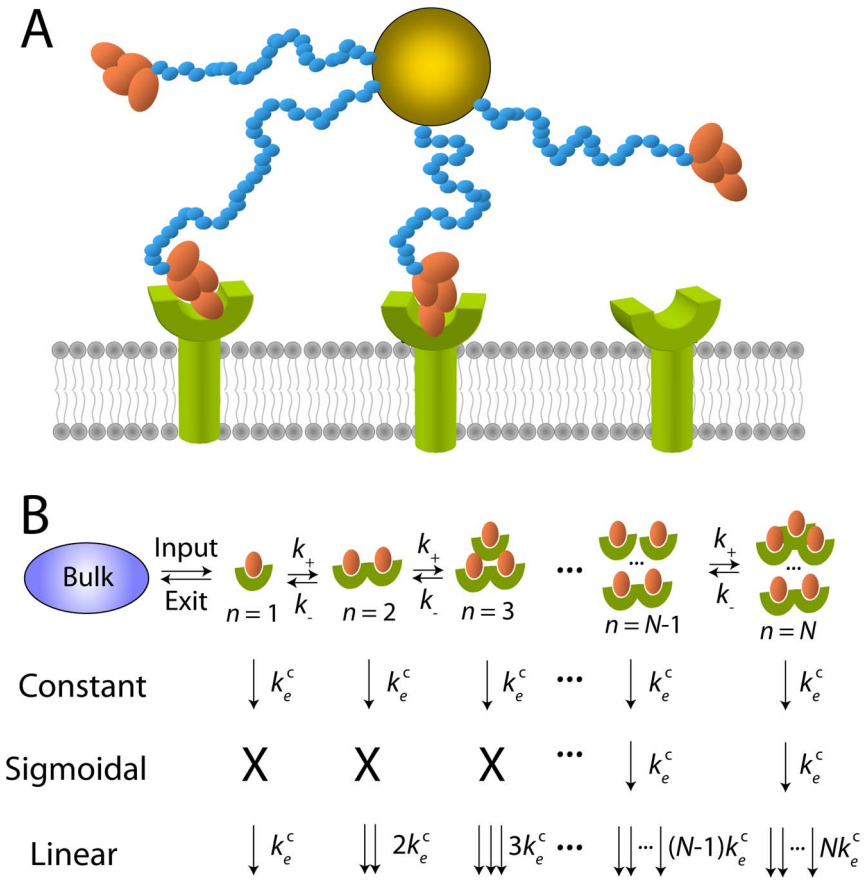

Figure 1. Schematic of model kinetics and endocytosis profiles. (A) Nanocarrier (gold) with two of four ligands bound on receptors (green). (B) Mapping to a 1D random walk with constant, sigmoidal, and linear profiles dictating rates of endocytosis in each ligand binding state n.
doi:10.1371/journal.pone.0065623.g001

identically unity, so as K_a increases, the maximum tends to approach $N=1$, with the discreteness of N setting the optimum at $N=2$ as K_a goes to infinity, a result that is confirmed by our analytics (File S1).

We next considered the effects of altering the functional form of the endocytosis profile. Figs. 2B and C show the specificities for the linear endocytosis profile

$$k_e(n)=2k_e^c n/(N+1), \tag{5}$$

and the sigmoidal endocytosis profile

$$k_e(n)=k_e^c\Theta(n-n_s), \tag{6}$$

where Θ is the Heaviside step function and n_s is the threshold value of n, respectively. The location of the global optimum is not significantly affected by the changes to the endocytosis profile. At steady state, specificity values are similar for constant and linear endocytosis, the latter of which models the scenario where each ligand-receptor binding event triggers an independent signaling cascade that has a finite probability of resulting in endocytosis. By contrast, for sigmoidal endocytosis, the magnitude of the optimal specificity is considerably enhanced. For this cooperative endocytosis requiring multiple binding events [18], specificity is so enhanced because endocytosis occurs only with nanocarriers in ligand-binding states whose relative abundances display the cumulative effects of selection at every step. For a fixed total number of ligands, Fig. 2D demonstrates that specificity sharply increases by orders of magnitude as the value of the threshold, n_s, required to trigger endocytosis increases. This effect is a direct consequence of the specificity depending on the kinetics of binding, unbinding, and endocytosis. These results indicate that targeting receptors that are endocytosed in a cooperative fashion can yield significant improvements in specificity.

We next examined the impact of varying drug-delivery protocols for a fixed constant endocytosis profile, again focusing on how the specificity S depends on the nanocarrier design parameters. Figs. 3A, B, and C show the specificity as a function of N and K_a for the steady state, single-dose, and pretargeted drug-delivery protocols, respectively. Remarkably, just as in Fig. 2, we observed a robust set of locally optimal solutions appearing in a continuous curve ranging from $N=2$ for $k_+ \gg k_-$ to large N for $k_+ \sim k_-$. The fact that this optimal regime appears to be conserved across different protocols suggests that generically optimal drug designs, independent of administration protocol, are possible. For the pretargeted drug-delivery protocol for the same conditions, one can also achieve very large specificities simply through an appropriate choice of collection time window Δt: changes in t_1 by a factor of $2-3$ can result in orders of magnitude improvement in specificity (Fig. 3D). It should also be noted that specificity is much more sensitive to t_1 and only weakly dependent on t_2.

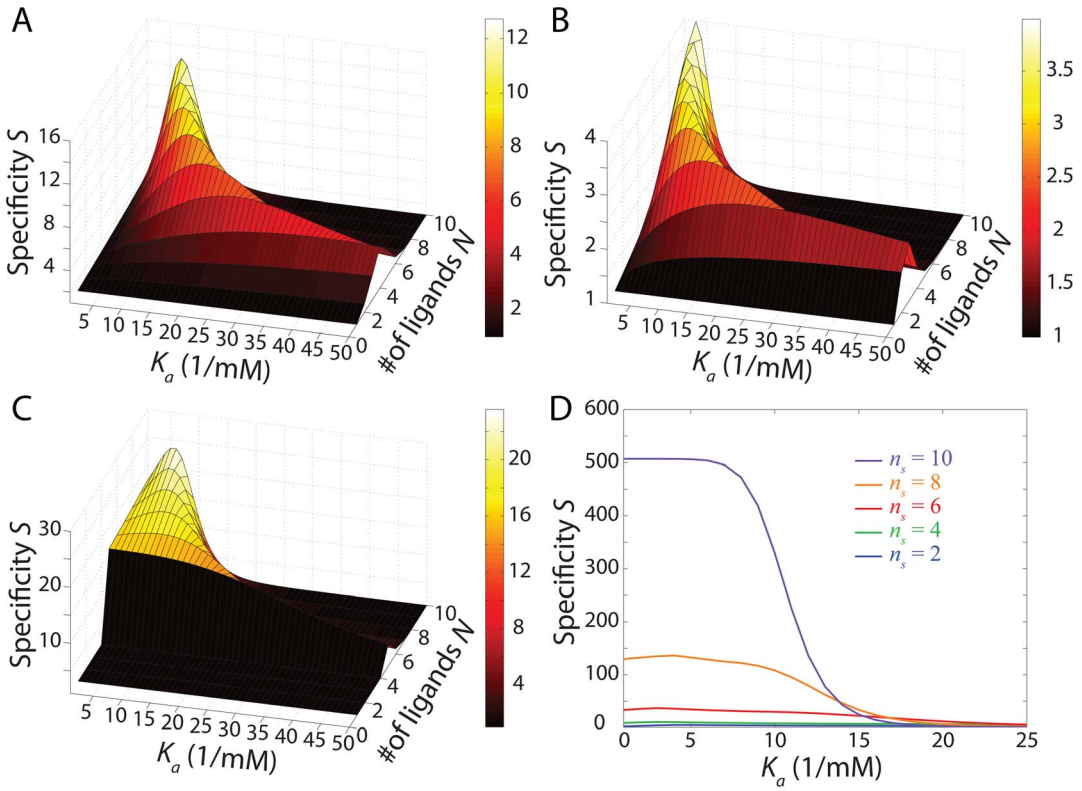

Figure 2. The endocytosis profile is a major determinant of specificity behavior. (A–C) Surface maps of specificity under the steady-state drug-delivery protocol with constant (A), linear (B), and sigmoidal endocytosis with $n_s = 5$ (C). (D) Maximum specificity under steady-state drug delivery and sigmoidal endocytosis for various threshold values. In all cases, the total number of ligands is $N = 10$, $k_e^c/k_- = 0.01$, and $\alpha = 2$.
doi:10.1371/journal.pone.0065623.g002

Multiplicative enhancement in specificity with optimal combination of drug-delivery protocol and endocytosis profile

Our results indicate that specificity can be significantly enhanced by independently tuning the drug-delivery protocol and the endocytosis profile via the choice of target receptor type. This suggests that judicious combinations of drug-delivery protocol and endocytosis profile coupled with appropriate design parameters could yield further increases in specificity. In Fig. 4A, we demonstrate this enhancement in the case of pretargeted drug delivery and sigmoidal endocytosis, for which we found a maximum specificity up to 10^4 times the value of the selectivity expected from the overexpression factor alone and over 300 times the specificity for the combination of steady-state delivery and constant endocytosis, which is the closest mimic to equilibrium conditions. The effect appears to be multiplicative, with only modest ($\sim 50-100$) increases expected due to cooperative endocytosis (Fig. 2D) or pretargeted delivery (Fig. 3D) alone.

While the optimal region was broadly consistent across protocols or endocytosis profiles when one or the other was fixed, we wished to ascertain whether this remained true for arbitrary combinations. Fig. 4B depicts the maximum specificities for all combinations of drug-delivery protocol and endocytosis profile. There is a clear clustering of the optimal solutions for all combinations along a region ranging from $N = 2$ for large K_a to large N for low K_a. While we explained the $N = 2$ optimum at large K_a, the global optimum for low K_a is of great interest. As discussed above, this regime should roughly correspond to the situation when a nanocarrier bound with one ligand to a cancer cell is marginally more likely to bind another ligand. This means $Nk_+ \sim k_-$ or $N \propto k_-/k_+ \sim 1/K_a$. With the asymptote at large K_a

Table 1. Typical parameter values.

Parameter	Symbol	Investigated values	Reported values
Overexpression factor	α	$2-20$	$1-292$ [22]
Endocytosis rate ($\sec^{-1}$)	k_e^c	$10^{-5}-10^{-1}$	$2\times10^{-4}-15$ [3]
Dissociation rate ($\sec^{-1}$)	k_-	0.1	0.1 [23]
Logarithmic dissociation constant*	pK_a	$2-10$	$2-15$ [24]**

*$pK_a = -\log_{10} K_a$, as measured for individual ligands.
**Multivalent complexes have been engineered with individual ligand $pK_a \approx 6$, and full complex $pK_a > 10$. [25]
doi:10.1371/journal.pone.0065623.t001

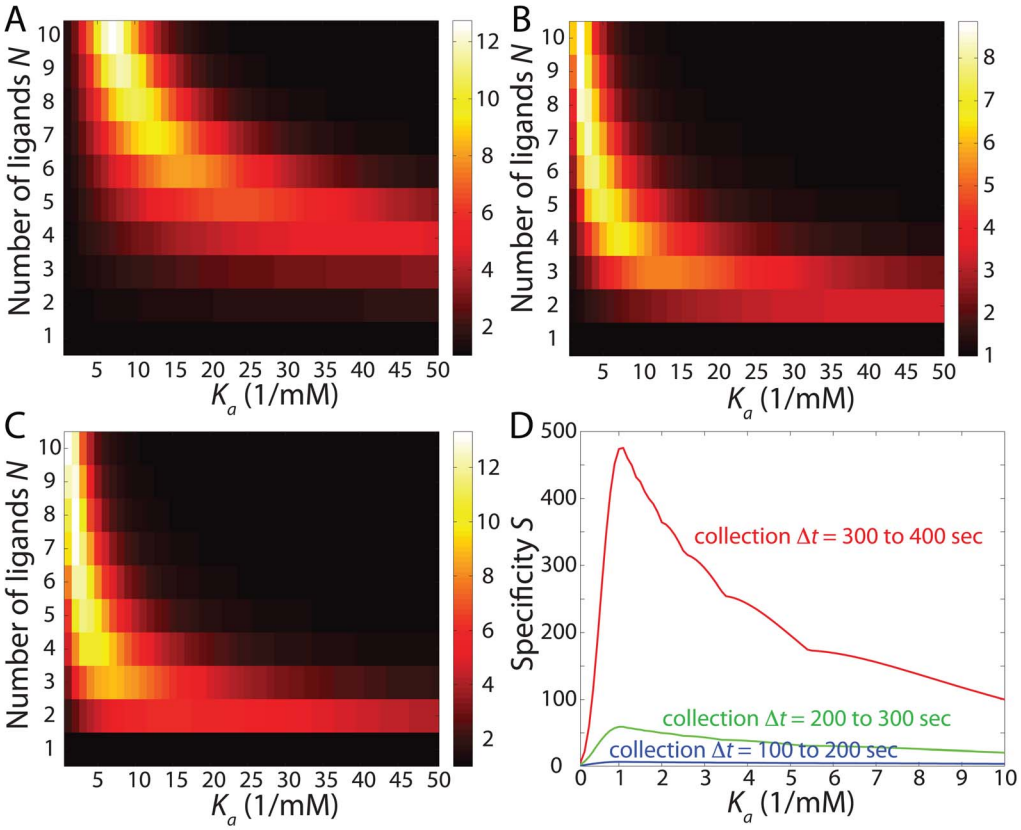

Figure 3. The drug-delivery protocol is also a major determinant of specificity behavior. (A–C) Specificity for a constant endocytosis profile under steady-state (A), single-dose (B), and pretargeted drug-delivery protocols (C). For the pretargeted drug-delivery protocol, the collection time window Δt is from 200 to 300 seconds. (D) Maximum specificity under the pretargeted drug-delivery protocol and constant endocytosis for various values of Δt. In all cases $k_e^c/k_- = 0.01$ and $\alpha = 2$.
doi:10.1371/journal.pone.0065623.g003

being $N = 2$, one arrives at the heuristic rule, $N \sim \beta/K_a + 2$, where β is a constant that depends on Δt, α, and k_e^c. Fig. 4B shows two such curves with different values of β for comparison.

Since the optimal design solutions and the corresponding specificities depend on α and k_e^c, we show those dependencies in Figs. 4C and D across drug-delivery protocols for a fixed constant endocytosis profile. The specificity rises sharply for a value of $\alpha = \alpha^*$ that is roughly constant across protocols. Since this value of α^* is set by the design parameters and choice of receptor (see File S1 for details), another strategy for achieving high specificity is to choose a receptor for which its typical overexpression factor is just above this value. This ensures that any cancer cells with $\alpha \gtrsim \alpha^*$ are targeted with high specificity. In fact, this was also identified as a mechanism for super-selectivity in equilibrium studies [16]. The kinetic effects of the drug-delivery protocol significantly affect the actual selectivity near α^*, with the pretargeted protocol having the largest specificity enhancement. Finally, we observed that the specificity generally decreases with increasing endocytosis rate (Fig. 4D), indicating that receptors that are being recycled more slowly are potentially better targets. This particular dependence might also arise in a very different context: the accelerated establishment of morphogen gradients in the presence of degradation, which can be described by similar equations [19].

Discussion

In conclusion, we have shown that specificity peaks occur as a function of both affinity and number of ligands, implying the existence of optimal nanocarrier designs. Overall, complexes with individual ligand K_d in the mM range ($pK_a \approx 3$) and large numbers of ligands per carrier have design features that yield high specificity in our simulations. This optimal region of the design parameter space is robust across drug-delivery protocols and endocytosis mechanisms. The precise specificity peak magnitude and sharpness can be customized through the careful selection of parameters or administration strategies. Possible strategies to increase specificity include targeting receptors that trigger endocytosis only if bound in groups and/or have a low overall endocytosis rate, and utilizing pretargeted drug delivery with long waiting times.

It should be noted that increased specificity comes at the cost of having a lower overall number of endocytosed nanocarriers. While we assumed that the dosage can be increased as necessary, in clinical practice there may be other factors such as the kidney's ability to clear the medication from the body that may limit the ability to maximize specificity. In order to address general design principles and strategies, we also chose to ignore a number of other specific system characteristics, including the possibility that α is time dependent, interactions between ligands, and details of the nanocarrier complex geometry (see File S1 for details).

Overall, our work complements equilibrium studies such as [16], by demonstrating that it is possible to design very high specificity complexes for non-equilibrium conditions. A specific advantage of our approach of using low-affinity multivalent nanocarriers is that it reduces the need for high-specificity ligands, which are usually of high molecular weight (such as antibody fragments) and can lead to drugs that have poor bioavailability

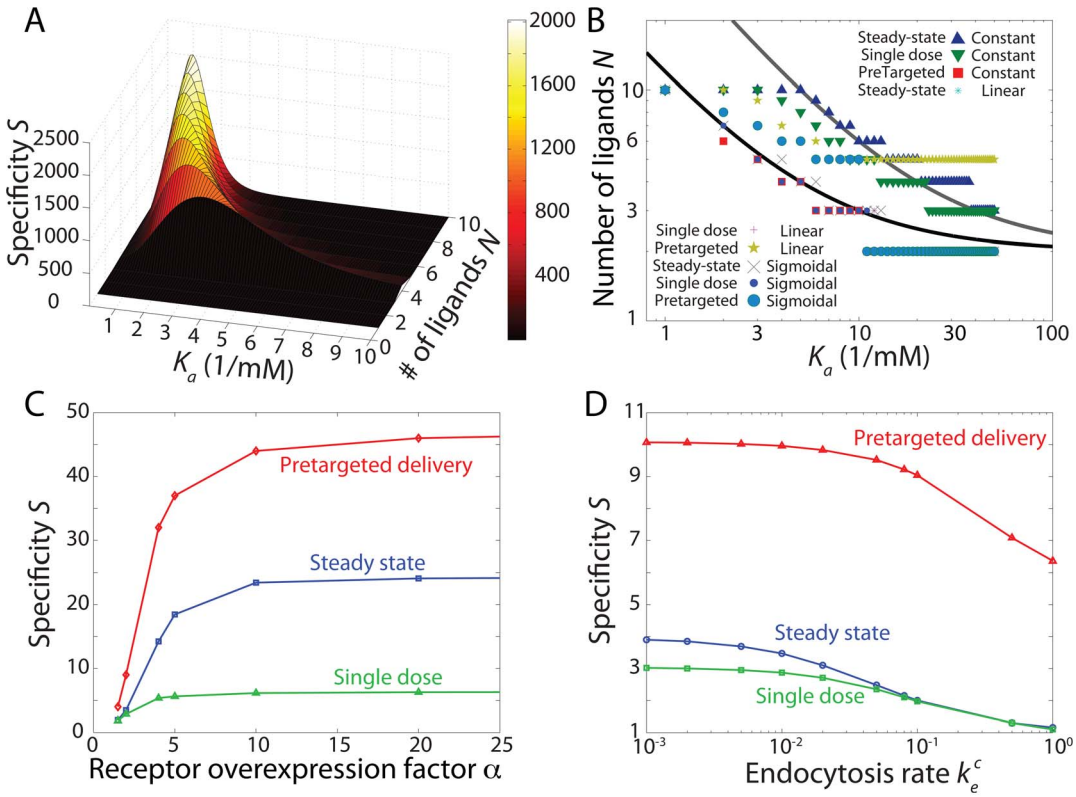

Figure 4. Specificity can be widely varied depending on parameter selection. (A) The combination of pretargeted drug-delivery protocol and sigmoidal endocytosis exhibits the highest specificity of all combinations examined. $k_e^c = 0.01$, $\alpha = 2$, threshold at $n = 5$. (B) Maximum specificity across all combinations. $k_e^c = 0.01/k_-$, $\alpha = 2$, $n_s = 5$ for sigmoidal endocytosis, and Δt from 200 to 300 sec for pretargeted drug-delivery protocol. Solid lines correspond to $\beta = 10$ and 30. (C) Effects of the overexpression factor α on specificity across drug-delivery protocols for constant endocytosis profile at $N = 8$, $K_a = 4/\mathrm{mM}$. The specificity rises sharply at $\alpha^* \approx 3$. (D) Effects of the endocytosis rate k_e^c (normalized by k_-) across drug-delivery protocols for constant endocytosis profile at $N = 8$, $K_a = 4/\mathrm{mM}$, $\alpha = 2$.
doi:10.1371/journal.pone.0065623.g004

[20]. It is to be noted that our work is not focused on a single biological system but rather addresses an entire class of biological, chemical, and bioengineering problems. By focusing on only physical quantities and not the specific chemical, biological, and clinical features of each possible system, we have derived broad, general, and overarching design principles. Our results can therefore potentially be applied to processes that trade off a few highly specific recognition sites versus a greater number of less specific sites; for example, to design a column to optimally separate chemicals or to design DNA sequences with an overrepresented number of certain motifs. It is also of interest to note that successive ligand-receptor binding reactions set up a multiple reaction step process similar to kinetic proofreading [21] that sharply increases the relatively low bias toward binding on cancer cells. Thus, as the number of steps increases, specificity can become very high. However, unlike in kinetic proofreading, energy is not expended to bias every reaction step, with the resulting cost being the overall reduction of nanocarrier endocytosis probability. Finally, given the ubiquity of multivalent low-affinity interactions and the inherently non-equilibrium environment in biology, it is possible that nature already exploits the mechanism we have discussed to gain significant improvements in specificity over the bounds dictated by equilibrium.

Supporting Information

File S1 Contains supporting information on assumptions in our model regarding receptor availability and ligand interdependence, rate dependencies, definitions of K_a and K_d, and an analytic solution of the master equations and determination of the specificity for the case of steady state with constant endocytosis profile. Figure S1, Surface plot of specificity S as a function of K_a and N, showing a ridge extending toward large values of K_a (out of the page). For fixed and large K_a, the specificity as a function of N has a peak at $N = 2$. Here, $k_e^c = 0.01$ and $\alpha = 3$. Figure S2, Crossover value of overexpression factor α^* as a function of affinity, K_a, and number of ligands, N (inset). $k_e = 0.01$ for both plots, $N = 10$ for the main plot and $K_a = 8/\mathrm{mM}$ for the inset. In general, α^* tends to qualitatively follow the behavior of the specificity S for the same parameter values.
(PDF)

Author Contributions

Conceived and designed the experiments: KT IG MEC KCH AG. Performed the experiments: KT IG. Analyzed the data: KT IG KCH AG. Contributed reagents/materials/analysis tools: KT IG KCH AG. Wrote the paper: KT IG KCH MEC AG.

References

1. Langer R (2001) Drugs on target. Science 293: 5527.
2. Perelson AS, Weisbuch G (1997) Immunology for physicists. Rev Mod Phys 69: 4.
3. Licata NA, Tkachenko AV (2008) Kinetic limitations of cooperativity-based drug delivery 210 systems. Phys Rev Lett 100: 158102.
4. Allen TM, Cullis PR (2004) Drug delivery systems: entering the mainstream. Science 303: 5665.
5. Baker M (2010) Rna interference: Homing in on delivery. Nature 464: 1225–1228.
6. Joshi A, Vance D, Rai P, Thiyagarajan A, Kane RS (2008) The design of polyvalent therapeutics. Chemistry 215 14: 7738–7747.
7. Peer D, Karp JM, Hong S, Farokhzad OC, Margalit R, et al (2007) Nanocarriers as an emerging platform for cancer therapy. Nat Nanotechnol 2: 751–760.
8. Rolland O, Turrin C-O, Caminade A-M, Majoral J-P (2009) Dendrimers and nanomedicine: multivalency in action. New J Chem 33: 1809–1824.
9. Badjic JD, Nelson A, Cantrill SJ, Turnbull WB, Stoddart JF (2005) Multivalency and cooperativity in supramolecular chemistry. Acc Chem Res 38: 723–732.
10. Kitov PI, Bundle DR (2003) On the nature of the multivalency effect: A thermodynamic model. J Am Chem Soc 125: 16271–16284.
11. Carlson CB, Mowery P, Owen RM, Dykhuizen EC, Kiessling LL (2007) Selective tumor cell targeting using 225 low-affinity, multivalent interactions. ACS Chem Biol 2: 119–127.
12. Wang S, Dormindontova EE (2011) Nanoparticle targeting using multivalent ligands: computer modeling. Soft Matter 7: 4435–4445.
13. Bartlett DW, Su H, Hildebrandt IJ, Weber WA, Davis ME (2007) Impact of tumor-specific targeting on the biodistribution and efficacy of sirna nanoparticles measured by multimodality in vivo imaging. Proc Natl 230 Acad Sci USA 104: 15549–15554.
14. Poirier C, van Effenterre D, Delord B, Johannes L, Roux D (2008) Specific adsorption of functionalized colloids at the surface of living cells: A quantitative kinetic analysis of the receptor-mediated binding. Biochim Biophys Acta 1778: 2450–2457.
15. Collins BE, Paulson JC (2004) Cell surface biology mediated by low affinity multivalent protein-ligand interactions. Curr Opin Chem 235 Biol 8: 617–625.
16. Martinez-Veracoechea FJ, Frenkel D (2011) Designing super selectivity in multivalent nano-particle binding. Proc Natl Acad Sci USA 108: 10963–10968.
17. Mulder A, Huskens J, Reinhoudt DN (2004) Multivalency in supramolucular chemistry and nanofabrication. Org Biomol Chem 2: 3409–3424.
18. Parton RG, Richards AA (2003) Lipid rafts and caveolae as portals for endocytosis: New insights and common mechanisms. Traffic 4: 724–728.
19. Kolomeisky AB (2011) Formation of a morphogen gradient: Acceleration by degradation. J Phys Chem Lett 2: 1502–1505.
20. Wu AM, Senter PD (2005) Arming antibodies: prospects and challenges for immunoconjugates. Nat 245 Biotechnol 23: 9.
21. Hopfield JJ (1974) Kinetic proofreading: A new mechanism for reducing errors in biosynthetic processes requiring high specificity. Proc Natl Acad Sci USA 71: 4135–4139.
22. Ross JF, Chaudhuri PK, Ratman M (1994) Differential regulation of folate receptor isoforms in normal and malignant tissues in vivo and in established cell lines. Cancer 73: 9.
23. Hlavacek WS, Percus JK, Percus OE, Perelson AS, Wofsy C (2002) Retention of antigen on follicular dendritic cells and b lymphocytes through complement-mediated multivalent ligand-receptor interactions: theory and application to hiv treatment. Math Biosci 176: 185–202.
24. Adams DJ, Morgan LR (2011) Tumor physiology and charge dynamics of anticancer drugs: Implications for camptothecin-based drug development. Curr Med Chem 18: 9.
25. Hong S, Leroueil PR, Majoros IJ, Orr BG, Baker JR Jr, et al (2007) The binding avidity of a nanoparticlebased multivalent targeted drug delivery platform. Chem Biol 14: 107.